

## LINEAR MODEL PREDICTIVE CONTROL STRATEGIES APPLIED TO A BATCH SUGAR CRYSTALLIZER

Luis Sánchez Dediós<sup>1</sup>, Petia Georgieva<sup>2\*</sup>, Sebastião Feyo de Azevedo<sup>1</sup>

<sup>1</sup> *Faculdade de Engenharia, Departamento de Engenharia Química, Universidade de Porto  
Rua Doutor Roberto Frias s/n*

<sup>2</sup> *Departamento de Electrónica & Telecomunicações IEETA, Universidade de Aveiro  
Campus Universitário de Santiago, 3810-193 Aveiro, Portugal, petia@det.ua.pt*

**Abstract:** The study of four structures of linear model predictive control (LMPC) for a batch white sugar crystallization process is reported in this paper. Two SISO and two MIMO control schemes were compared with respect to the final process quality achieved. The linear models required in the controller structures were extracted applying two identification alternatives. The SISO cases seem to guarantee more satisfactory end point quality of the process. However, only the LMPC of the supersaturation manipulating the steam flowrate makes feasible all conflicting control objectives.

*Copyright 2006 CONTROLO*

**Keywords:** generalized model predictive control, batch crystallization process, input-output linear model identification

### 1. INTRODUCTION

During the last decade the model based predictive control (MPC) became an attractive control strategy implemented in a variety of process industries. However, it can be considered as industrial alternative only for continuous and predominantly linear processes (Qin and Badgwell, 2003). The application of MPC for batch nonlinear cases is still far from being an industrial reality and represents an interesting theoretical and practical control challenge (Balasubramhanya and Doyle, 2000). The batch or fed-batch mode is a typical production scheme for a large group of pharmaceutical, biotechnological, food and chemical processes. It is related with the formulation of a control problem in terms of economic or performance objective at the end of the process (Nagy and Braatz, 2003). For example, the crystallisation quality is evaluated by the particle size distribution (PSD) at the end of the process which is quantified by two parameters - the final average (in mass) particle size (MA) and the final coefficient of particle variation (CV). The main challenge of the batch production is the large batch to batch variation of the final PSD. This lack of process repeatability is caused mainly by improper control policy and results in product recycling and loss increase. MPC, being one of the approaches that inherently can cope with process constraints, nonlinearities, and different objectives derived from economical or environmental

considerations (Morari and Lee, 1997), has the potential to overcome the problem of the lack of repeatability and drive the process to its optimal state of profit maximization and cost minimization.

The present work is focused on a comparative analysis between various scenarios of linear MPC implemented to a batch white sugar crystallizer. Two Single Input Single Output (SISO) and two Multiple Input Multiple Output (MIMO) MPC schemes were compared with respect to the final process quality achieved. The linear models required in the controller structures were extracted applying two identification approaches – classical (one test) and double test identification. The SISO scheme with a double test identified model seem to guarantee more satisfactory end point quality of the process. However, only one of the tested linear MPC scenarios (controlled output – supersaturation, manipulated input - steam flowrate) makes feasible all conflicting control objectives.

### 2. DESCRIPTION OF THE PROCESS

Sugar crystallisation occurs through the mechanisms of nucleation, growth and agglomeration. The impact of operating conditions on these activities is not always well understood. The process is characterised by strongly non-linear and non-stationary dynamics

and can be divided into the following sequential phases.

**Charging.** During the first phase (about 20 min.) the pan is partially filled with a juice containing dissolved sucrose (termed liquor). The initial liquid charged in the pan has to cover completely the calandria at the bottom and should be kept at least 12.6 cm. above it. This corresponds to approximately 40% of the total vessel height. Therefore, the charge is performed by opening the feeding valve to a maximum point and charging until the level sensor indicates 40%. According to the relation between the level ( $L$ ) and the volume of the solution ( $V_{sol}^{init} (m^3) = 0.405(L(\%) - 10)$ ) the level reached corresponds to a volume of 12.15  $m^3$ .

**Concentration.** The next phase is the concentration. The liquor is concentrated by evaporation, under vacuum, until supersaturation reaches a predefined value (typically 1.11). At this stage seed crystals are introduced into the pan to induce the production of crystals. This is the beginning of the third (crystallisation) phase.

**Crystallisation (main phase).** In this phase as evaporation takes place further liquor or water is added to the pan in order to guarantee crystal growth at a controlled supersaturation level and to increase total contents of sugar in the pan. Near to the end of this phase and for economical reasons, the liquor is replaced by other juice of lower purity (termed syrup).

**Tightening.** The fourth phase consists of tightening which is principally controlled by evaporation capacity. The pan is filled with a suspension of sugar crystals in heavy syrup, which is dropped into a storage mixer. At the end of the batch, the final massecuite undergoes centrifugation, where final refined sugar is separated from (mother) liquor that is recycled to the process.

The different phases are comparatively independent process states and since the crystallisation is the main stage responsible for the final product quality in terms of PSD, this study is focused on analysing several LMPC strategies specifically for the crystallization phase.

Based on a set of industrial data collected over normal white sugar production cycles, average values for the main process variables were determined and summarised in Table 1. Table 2 consists of the reference values and restrictions of the process quality variables evaluated at the batch end ( $t_f$ ).

The supersaturation is the main driving force of the crystallization but the actual measured variable is the brix of the solution. However, due to a straightforward relation between supersaturation and brix, the supersaturation is considered as the controlled process output. For more details with respect to the process see Georgieva, *et al.*, 2003.

Table 1. Process variables

| Name                       | Notation   | Average values       |
|----------------------------|------------|----------------------|
| Liquor/Syrup feed flowrate | $F_f$      | 0.0057 $m^3 / s$     |
| Steam flowrate             | $F_s$      | 1.6 $m^3 / s$        |
| Water feed flowrate        | $F_w$      | 0 $m^3 / s$          |
| Feed temperature           | $T_f$      | 65 °C                |
| Steam temperature          | $T_s$      | 140 °C               |
| Brix of feed               | $Bx_f$     | 0.7 [ ]              |
| Steam pressure             | $P_s$      | 2 bar                |
| Temperature of massecuite  | $T_m$      | 72.4944 °C (average) |
| Vacuum pressure            | $P_{vac}$  | 0.25 bar             |
| Brix of the solution       | $Bx_{sol}$ | 2 bar (average)      |
| Stirring power             | $W$        | 15000 W              |

Table 2. Reference values and restrictions of process quality variables

| Name                           | Notation   | Value             |
|--------------------------------|------------|-------------------|
| $t_f$ - final time             |            |                   |
| Average (in mass) crystal size | $AM(t_f)$  | 0.5-0.6 mm (ref.) |
| Coeff. of variation            | $CV(t_f)$  | below 25%         |
| Volume                         | $V(t_f)$   | 35 $m^3$ (max)    |
| Supersaturation                | $S$        | 1.3 (max)         |
| Mass fraction of crystals      | $w_c(t_f)$ | 40 % (min)        |

### 3. IDENTIFICATION STRATEGIES

Attempts to extract a representative linear model describing all phases of the process, from charging to centrifugation, are most likely to fail. However, looking for a reliable linear approximation only for the crystallization phase is worth to study. The general structure of the input-output linear model assumed for identification has the following mathematical representation (Rossiter, 2003):

$$y(t) = \sum_{i=1}^{n_u} \frac{B_i(q^{-1})}{A_i(q^{-1})} u_i(t) + e(t) \quad (1)$$

where  $n_u$  is the number of model inputs. The orders of the numerator  $B_i(q^{-1})$  and the denominator  $A_i(q^{-1})$  are  $n_b$  and  $n_a$  respectively, which means  $(n_b+n_a)$  parameters are to be adjusted.

The first identification step is to specify the model inputs and outputs. The main candidates are those process variables that mainly influence the final product quality. The feed flowrate, steam flowrate and vacuum pressure are usually the manipulated physical inputs in the crystallization industry and therefore they are considered as possible model inputs. As for the outputs, the supersaturation, being the driving force for the crystallization phenomenon, the temperature of the massecuite and the average in

mass crystal size (AM) are the most important control variables and are assumed as possible model outputs.

The choice of  $n_b$  and  $n_a$  is crucial in terms of model reliability, complexity and sensitivity. Their final values were chosen after a number of tests minimizing the Relative Mean Square (RMS) error defined as follows:

$$RMS_i = \sqrt{\frac{\sum_{k=1}^N (y_{ik}^r - y_{ik}^m)^2}{\sum_{k=1}^N (y_{ik}^r)^2}} \quad (2)$$

Where  $y_i^r$  are the data related to a process variable considered as the output  $i$ ,  $y_i^m$  is the respective model output  $i$ ,  $k$  is the sampling instant and  $N$  is total number of samples.

In the identification tests, the inputs are generated as random variations limited by maximum of 10% around the average values collected in Table 1. The inputs were simulated, in Matlab, as pseudo-random binary signals (PRBS) invoking the Simulink signal builder. The sampling period was fixed as 30 sec.

**Remark:** For the second half of the crystallization the random generation policy applied to the feed flow rate of syrup led to a very small quantity of masecuite at the phase end. Therefore the identification proceeded with empirically determined feed flow rate such that the final volume approaches the respective reference value given in Table 2. Two identification strategies were investigated.

### 3.1 Classical (one test) identification

The randomly generated inputs ( $u_i$ ) are introduced either to the process (if experiments with the process are allowed), or to a very detailed process model that simulate the process (the case in this work). The process responses are recorded ( $y_i$ ) and the respective mean values are computed ( $u_{i,mean}$ ,  $y_{i,mean}$ ). Then the coefficients of the linear model (1) are extracted supplying as inputs  $u_i - u_{i,mean}$  and as outputs  $y_i - y_{i,mean}$ . This classical identification requires only one test for identification as it is illustrated in Fig. 1 for the case of two inputs and two outputs ( $i = 1, 2$ ).

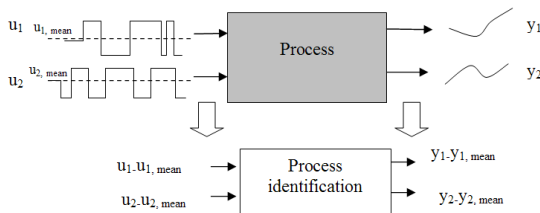


Fig. 1 Classical (one test) identification

### 3.2 Double test identification

An alternative of the so-called classical identification is proposed here where prior to the test with randomly generated inputs ( $u_i$ ), a test with constant inputs ( $u_i' = u_{i,mean}$ ) is performed and the process reactions ( $y_i, y_i'$ ) are recorded, see Fig. 2. Next, the coefficients of the linear model (1) were extracted supplying as inputs  $u_i - u_i'$  and as outputs  $y_i - y_i'$ .

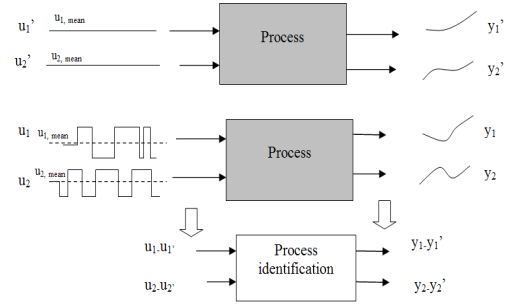


Fig. 2 Double-test identification

This double test identification requires more computational efforts than the classical approach, but has the potential to provide a better approximation.

**Remark:** Instead of constant inputs, base input trajectories might be used as an alternative solution for the first test.

## 4. MPC –PROBLEM FORMULATION

Linear MPC is an optimisation-based multivariable constrained control technique that uses a linear dynamic model for the prediction of the process outputs. At each sampling time the linear model predicts future process responses to potential control signals over the prediction horizon ( $H_p$ ). The predictions are supplied to an optimization procedure to determine the values of the control action over a specified control horizon ( $H_c$ ) that minimize the following performance index

$$\min_{u_{\min} \leq [u_k, u_{k+1}, \dots, u_{H_c}] \leq u_{\max}} P = \lambda_1 \sum_{k=1}^{H_p} (r_k - y_k^m)^2 - \lambda_2 \sum_{k=1}^{H_c} (u_{k-1} - u_{k-2})^2 \quad (3)$$

The prediction horizon  $H_p$  is the number of time steps over which the prediction errors are minimized and the control horizon  $H_c$  is the number of time steps over which the control increments are minimized,  $r$  is the desired response (the reference) and  $y^m$  is the model response.  $u_k, u_{k+1}, u_{H_c}$  are tentative future values of the control input, which are limited by  $u_{\min}$  and  $u_{\max}$  and parameterized as piece wise constant.  $\lambda_1$  and  $\lambda_2$  are the output and the input weights respectively, which determine the contribution of each of the components (the output error and the control increments) of the performance index (3). The length of the prediction horizon is

crucial for achieving tracking and stability. For small values of  $H_p$  the tracking deteriorates but for high  $H_p$  values the bang-bang behaviour of the process input might be a real problem. The MPC controller requires a significant amount of on-line computation, since the optimization (3) is performed at each sample time to compute the optimal control input. At each step only the first control action is implemented to the process.

## 5. SISO MPC STRUCTURES

Single Input Single Output (SISO) MPC based on a linear process model is the first control strategy to consider. The control objective is to get a high quality final product which is quantified by a desired final average crystal size,  $AM(t_f)$ , by minimisation of the final coefficient of variation,  $CV(t_f)$  and by maximisation of the final crystal content  $w_c(t_f)$ . This end point quality is going to be achieved by two different structures depending on the selected control input, manipulating the feed flowrate (Structure 1) or the steam flowrate (Structure 2), such that the supersaturation follows a previously determined (by an optimization scheme) reference trajectory (see Georgieva and Feyo de Azevedo, 2006 for more details).

The aim of this study is also to analyse the influence of the two identification approaches discussed in section 3. Therefore, for each of the two SISO control structures, the model obtained by classical identification and the model obtained by double test identification were implemented.

### 5.1 MPC of supersaturation manipulating feed flowrate.(Structure 1)

The results of five tests for MPC of the supersaturation manipulating the feed flowrate (Structure 1) are summarized in Table 3 and Table 4. The model (1) is obtained either by classical identification (in Table 3) with  $n_b=5$  and  $n_a=7$  or by doublet test identification (in Table 4) with  $n_b=4$  and  $n_a=7$ . In both cases the selected polynomial degrees guaranteed an RMS error below 0.1. The identified parameters of the models are included in the Appendix. The control sampling time was chosen to be equal to the identification sampling time,  $T_s = 30s$  and  $\lambda_1 = 1$ . The effect of varying the main controller parameters  $H_p$ ,  $H_c$  and  $\lambda_2$  is studied. The prediction horizon is either shifted by usually one sampling time into the future or *shrunk* (Nagy *et al.*, 2005) in case it was initially equal to the batch duration. Hence, the shrunk  $H_p$  or  $H_c$  is calculated as follows:

$$N_{shrunk} = \frac{(t_f - t_{actual})}{T_s} \quad (4)$$

Where  $t_f$  is the final time and  $t_{actual}$  is the current time. In the first three columns of Table 3 and 4, the effect of increasing the prediction horizon ( $H_p$ ) and keeping

constant the control horizon ( $H_c$ ) is studied. Note that it improves the end point objectives  $AM(t_f)$  and  $w_c(t_f)$  but to the expense of worse  $V(t_f)$ . Applying eq. (4) to determine the shrunk prediction horizon (column 4) and control horizon (column 5) has the effect of reducing the input weight  $\lambda_2$  in (3) to get the desired final time values of the quality variables.

Table 3. MPC (Structure 1) with model obtained by classical identification

| Case        | 1     | 2     | 3     | 4      | 5       |
|-------------|-------|-------|-------|--------|---------|
| $H_c$       | 5     | 5     | 5     | 5      | Shrunk. |
| $H_p$       | 5     | 6     | 10    | Shrunk | Shrunk  |
| $\lambda_2$ | 10    | 10    | 10    | 1      | 1       |
| $S_{max}$   | 1.21  | 1.21  | 1.21  | 1.19   | 1.21    |
| $AM(t_f)$   | 0.47  | 0.50  | 0.59  | 0.44   | 0.59    |
| $CV(t_f)$   | 23.29 | 23.34 | 23.40 | 23.29  | 23.39   |
| $V(t_f)$    | 30.58 | 28.62 | 24.33 | 32.18  | 24.27   |
| $w_c(t_f)$  | 0.43  | 0.46  | 0.55  | 0.40   | 0.55    |

Table 4. MPC (Structure 1) with model obtained by double-test identification

| Case        | 1     | 2     | 3     | 4      | 5      |
|-------------|-------|-------|-------|--------|--------|
| $H_c$       | 5     | 5     | 5     | 5      | Shrunk |
| $H_p$       | 5     | 6     | 10    | Shrunk | Shrunk |
| $\lambda_2$ | 10    | 10    | 10    | 1      | 1      |
| $S_{max}$   | 1.21  | 1.21  | 1.20  | 1.31   | 1.31   |
| $AM(t_f)$   | 0.49  | 0.50  | 0.62  | 0.47   | 0.48   |
| $CV(t_f)$   | 23.34 | 23.37 | 23.42 | 21.42  | 21.40  |
| $V(t_f)$    | 28.94 | 28.29 | 23.47 | 35.28  | 34.89  |
| $w_c(t_f)$  | 0.46  | 0.47  | 0.57  | 0.35   | 0.36   |

### 5.2 MPC of supersaturation manipulating steam flowrate (Structure 2)

The same tests, as in the previous subsection, for MPC of supersaturation are summarised in Table 5 and Table 6 but now manipulating the steam flowrate (Structure 2). The linear models were obtained again by classical identification (in Table 5) with  $n_b=5$  and  $n_a=7$  and by double test identification (in Table 6) with  $n_b=4$  and  $n_a=7$ . The identified parameters are listed in the Appendix (section A1). The general conclusion is that the MPC scheme with model based on the classical identification cannot guarantee sufficient quality with respect to  $AM(t_f)$  and  $w_c(t_f)$ . Note that for no one of the five cases considered the conflicting end point objectives are simultaneously feasible.

In contrast to the above conclusions, the MPC scheme with model based on the double-test identification, gives quite stable and not sensible, to small control parameter changes, results. In fact, this is the only scheme where all conflicting end point objectives are simultaneously feasible for all cases (see Table 6).

## 6. MIMO MPC STRUCTURES

Multiple Input Multiple Output (MIMO) MPC based on a linear process model is the second control strategy considered. Our study is limited for the structure of two inputs - two outputs (TITO).

Table 5. MPC (Structure 2) with model obtained by classical identification

| Case         | 1     | 2     | 3     | 4      | 5      |
|--------------|-------|-------|-------|--------|--------|
| $H_c$        | 5     | 5     | 5     | 5      | Shrunk |
| $H_p$        | 5     | 5     | 15    | Shrunk | Shrunk |
| $\lambda_2$  | 1     | 0.1   | 1     | 1      | 1      |
| $S_{max}$    | 1.20  | 1.20  | 1.13  | 1.19   | 1.19   |
| AM ( $t_f$ ) | 0.47  | 0.45  | 0.14  | 0.32   | 0.32   |
| CV( $t_f$ )  | 22.78 | 22.80 | 5.01  | 22.78  | 22.89  |
| V( $t_f$ )   | 35.33 | 34.82 | 35.45 | 35.21  | 35.01  |
| $w_c(t_f)$   | 0.39  | 0.38  | 0.02  | 0.27   | 0.27   |

Table 6. MPC (Structure 2) with model obtained by double-test identification

| Case         | 1       | 2       | 3       | 4       | 5       |
|--------------|---------|---------|---------|---------|---------|
| $H_c$        | 5       | 5       | 5       | 5       | Shrunk  |
| $H_p$        | 5       | 5       | 15      | Shrunk  | Shrunk  |
| $\lambda_2$  | 1       | 0.1     | 1       | 1       | 1       |
| $S_{max}$    | 1.2005  | 1.1881  | 1.1928  | 1.195   | 1.1833  |
| AM ( $t_f$ ) | 0.4811  | 0.5373  | 0.5252  | 0.5305  | 0.5292  |
| CV( $t_f$ )  | 22.7992 | 23.1684 | 22.9758 | 23.5287 | 23.1891 |
| V( $t_f$ )   | 35.1066 | 34.8621 | 35.174  | 34.7471 | 34.9551 |
| $w_c(t_f)$   | 0.402   | 0.4655  | 0.4442  | 0.4735  | 0.4582  |

Due to the restricted space of the paper only two, of the various TITO structures tested, are reported, i) MPC of the supersaturation and the temperature of massequite manipulating the feed flow rate and the vacuum pressure (Structure 3) and ii) MPC of the supersaturation and the final value of AM manipulating the same inputs (Structure 4). Based on the encouraging results with the double test identification of the SISO models, now TITO linear models obtained only by double test identification are considered. The generalized input-output model structure has the following mathematical representation

$$\begin{aligned} A_1(z^{-1})y_1(t) &= B_{11}(z^{-1})u_1(t-1) + B_{12}(z^{-1})u_2(t-1) \\ A_2(z^{-1})y_2(t) &= B_{21}(z^{-1})u_1(t-1) + B_{22}(z^{-1})u_2(t-1) \end{aligned} \quad (5)$$

where the identified polynomials  $A_i$  and  $B_{ij}$  for each of the two structures are summarised in the Appendix (section A2).

### 6.1 MPC of supersaturation and temperature manipulating feed flow rate and vacuum pressure (Structure 3)

The final control objectives (the same as for the SISO cases), are to get a high quality final product quantified by the AM ( $t_f$ ), CV( $t_f$ ) and  $w_c(t_f)$ . However, the operational control objectives are different for each of the structures. For Structure 3 the aim is by manipulating simultaneously the feed flowrate and the vacuum pressure, to force the supersaturation and the temperature of massequite to follow reference trajectories. Results of the MPC applied to the two structures are summarised in Table 7 and 8. The input and output weights were chosen (by trial and errors) to compensate the different ranges of the two inputs and the two outputs respectively and to determine their different contribution to the performance index. Structure 3 and Structure 4 seem to be equally not sensitive to variations in controller parameters. The values of the final quality variables in the two structures are quite similar. This can be explained only with the clear priority of the supersaturation as the main controlled variable for the two structures. The temperature of massequite and the end value of AM have less influence on the optimal value of (3).

Table 7. Results of MIMO MPC (Structure 3)

| Case           | 1           | 2           | 3           | 4           |
|----------------|-------------|-------------|-------------|-------------|
| $H_c$          | 5           | 5           | 5           | 5           |
| $H_p$          | 5           | 15          | 30          | Shrunk      |
| Input Weights  | [ $10^4$ 1] | [ $10^4$ 1] | [ $10^4$ 1] | [ $10^4$ 1] |
| Output Weights | [ $10^3$ 1] | [ $10^3$ 1] | [ $10^3$ 1] | [ $10^3$ 1] |
| $S_{max}$      | 1.23        | 1.225       | 1.221       | 1.221       |
| AM ( $t_f$ )   | 0.46        | 0.434       | 0.434       | 0.441       |
| CV( $t_f$ )    | 23.30       | 23.112      | 23.03       | 23.016      |
| V( $t_f$ )     | 33.58       | 34.840      | 34.84       | 34.947      |
| $w_c(t_f)$     | 0.40        | 0.374       | 0.372       | 0.376       |

### 6.2 MPC of supersaturation and AM ( $t_f$ ) manipulating feed flow rate and vacuum pressure (Structure 4)

The operational goals, for Structure 4, are obtained by manipulating simultaneously the feed flowrate and the vacuum pressure, to force the supersaturation to follow a reference trajectory and to get a referenced final AM value. Note that in both structures (Structure 3 and Structure 4) the final AM and the final crystal content are slightly below the desired values and in all cases the results are worse than in Structure 2 (SISO MPC of supersaturation manipulating the steam flowrate). This result goes beyond theoretical proofs and can be interpreted with a significant discrepancy between the linear model part of the MPC structure and the inevitably nonlinear nature of the process in hand.

## 7. CONCLUSIONS

The study of two SISO and two MIMO cases of MPC with linear process model for a batch sugar crystallizer is shortly reported in this work. The

conditions of all experiments performed are summarised in Tables 1 and 2 and the linear models are extracted by the process simulator developed in Georgieva, *et al.*, 2003. The SISO cases seem to guarantee more satisfactory end point quality of the process. However, only the MPC of supersaturation manipulating the steam flowrate (Structure 2) makes feasible all conflicting objectives. Improved results are expected with a nonlinear model in the MPC scheme, which is not discussed in this paper but work on it is now in progress.

Table 8 Results of MIMO MPC (Structure 4)

| Case           | 1            | 4             | 3             | 4             |
|----------------|--------------|---------------|---------------|---------------|
| $H_c$          | 5            | 5             | 5             | 5             |
| $H_p$          | 5            | Shrunk        | Shrunk        | Shrunk        |
| Input Weights  | $[10^4 \ 1]$ | $[10^4 \ 10]$ | $[10^4 \ 10]$ | $[10^4 \ 10]$ |
| Output Weights | $[10^3 \ 1]$ | $[10^3 \ 1]$  | $[10^3 \ 1]$  | $[10^3 \ 1]$  |
| $S_{max}$      | 1.225        | 1.196         | 1.196         | 1.203         |
| AM ( $t_f$ )   | 0.456        | 0.433         | 0.433         | 0.466         |
| CV ( $t_f$ )   | 23.238       | 23.008        | 23.008        | 22.305        |
| V ( $t_f$ )    | 35.23        | 34.679        | 34.679        | 34.798        |
| $w_c(t_f)$     | 0.392        | 0.374         | 0.374         | 0.37          |

## 8. APPENDIX

### A1. SISO linear model, eq. (1):

a) Classical identification of SISO linear model of Structure 1

$$A=[1.0 \ -1.517 \ 0.4377 \ 0.377 \ -0.035 \ -0.697 \ 0.4453]$$

$$B=[-0.2465 \ 0.1597 \ 0.0246 \ -0.1982 \ 0.1118]$$

b) Double-test identification of SISO linear model of Structure 1

$$A=[1.0 \ -1.476 \ 0.172 \ 0.376 \ -0.157 \ 0.069 \ 0.0243]$$

$$B=[-0.0934 \ 0.1005 \ 0.0055 \ -0.0097]$$

c) Classical identification of SISO linear model of Structure 2

$$A=[1.0 \ -2.297 \ 1.743 \ -1.055 \ 1.119 \ -0.557 \ 0.0469]$$

$$B=[-0.0017 \ 0.0077 \ -0.0145 \ 0.0114 \ -0.0032]$$

d) Double-test identification of SISO linear model of Structure 2

$$A=[1.0 \ -0.0027 \ -1.061 \ -0.47 \ 0.016 \ 0.4 \ 0.1551]$$

$$B=[0.0054 \ 0.0040 \ -0.0049 \ -0.0034]$$

### A2. MIMO linear model, eq. (5):

a) MIMO linear model of Structure 3

$$A_1=[1.0 \ -3.628 \ 5.03 \ -3.6 \ 1.8 \ -0.673 \ -0.036 \ 0.11]$$

$$A_2=[1.0 \ -3.565 \ 4.902 \ -3.734 \ 2.4897 \ -1.677 \ 0.785 \ -0.31 \ 0.139 \ -0.038 \ 0.008]$$

$$B_{11}=[-0.1885 \ 0.4620 \ -0.3854 \ 0.1956 \ -0.1205 \ 0.0230 \ 0.0060 \ 0.0077]$$

$$B_{12}=[-0.036 \ 0.076 \ -0.019 \ -0.041 \ 0.014 \ 0.006]$$

$$B_{21}=[-2.2741 \ 6.4485 \ -6.2353 \ 2.6879 \ -1.2478 \ 0.8353 \ -0.2772 \ 0.0627]$$

$$B_{22}=[2.2235 \ -7.2479 \ 9.9931 \ -9.0508 \ 6.5667 \ -3.4479 \ 1.4080 \ -0.5101 \ 0.0651]$$

b) MIMO linear model of Structure 4

$$A_1=[1.0 \ -3.628 \ 5.03 \ -3.5997 \ 1.8 \ -0.673 \ -0.036 \ 0.107]$$

$$A_2=[1.0 \ -6.273 \ 16.87 \ -25.29 \ 22.9577 \ -12.7801 \ 4.1765 \ -0.7017 \ 0.0409]$$

$$B_{11}=[-0.19 \ 0.46 \ -0.39 \ 0.2 \ -0.12 \ 0.02 \ 0.01 \ 0.007]$$

$$B_{12}=[-0.036 \ 0.076 \ -0.019 \ -0.041 \ 0.014 \ 0.006]$$

$$B_{21}=[0.0805 \ -0.3311 \ 0.4927 \ -0.2656 \ -0.0593 \ 0.1202 \ -0.0405 \ 0.0031] * 10^{-3}$$

$$B_{22}=[0.209 \ -0.7085 \ 0.7199 \ 0.2729 \ -1.2363 \ 1.1405 \ -0.4754 \ 0.0779] * 10^{-3}$$

### ACKNOWLEDGMENT

This work was financed by the Portuguese Foundation for Science and Technology within the activity of the Research Units IEETA and ISR -Porto, which is gratefully acknowledged.

### REFERENCES

- Balasubramhanya, L.S., Doyle III, F.J. Nonlinear model-based control of a batch reactive distillation column. *Journal of Process Control*, **Vol. 10** (2000) 209-218
- Georgieva, P., Meireles, M.J., Fayo de Azevedo, S. Knowledge-based hybrid modelling of batch crystallization when accounting for nucleation, growth and agglomeration phenomena. *Chemical Engineering Science* **Vol. 58** (2003) 3699 – 3713.
- Georgieva, P., Fayo de Azevedo, S. Application of ANNs in modelling and optimization of batch crystallization processes, *Journal of DETI*, University of Aveiro, 2006 (to appear).
- Nagy, Z.K., Mahn, B., Franke, R., Allgöwer, F. Nonlinear model predictive control of batch processes: An industrial case study. *IFAC World Congress*, Prague, 4-8 July, 2005.
- Nagy, Z.K. and R.D. Braatz (2003). Robust nonlinear model predictive control of batch processes. *AIChE J.*, **49**, 1776-1786.
- Morari, M. and J.H. Lee (1997). Model predictive control: Past, present and future. In *Proc. PSE'97-ESCAPE-7 Symposium*, Trondheim.
- Rossiter J.A., *Model-based predictive control: a practical approach*, CRC press, June 2003, ISBN 0-9493-1291-4
- Qin S. J., and T. Badgwell (2003). A Survey of Industrial Model Predictive Control Technology. *Control Engineering Practice*, **11**, 733-764.